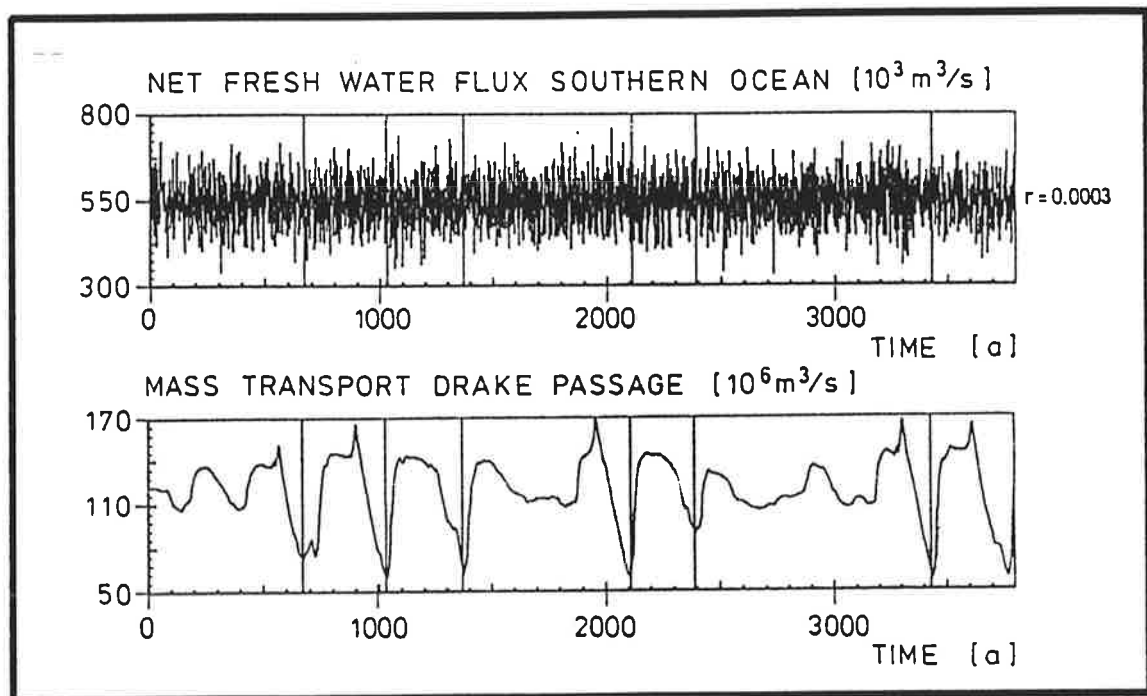




Max-Planck-Institut für Meteorologie

REPORT No. 50



INTERNAL SECULAR VARIABILITY IN AN OCEAN GENERAL CIRCULATION MODEL

by

U. MIKOLAJEWICZ • E. MAIER-REIMER

HAMBURG, MARCH 1990

AUTHORS:

UWE MIKOLAJEWICZ

MAX-PLANCK-INSTITUT
FUER METEOROLOGIE

ERNST MAIER-REIMER

MAX-PLANCK-INSTITUT
FUER METEOROLOGIE

MAX-PLANCK-INSTITUT
FUER METEOROLOGIE
BUNDESSTRASSE 55
D-2000 HAMBURG 13
F.R. GERMANY

Tel.: (040) 4 11 73-0
Telex: 211092
Telemail: MPI.Meteorology
Telefax: (040) 4 11 73-298

Internal secular variability in an ocean general
circulation model

by

Uwe Mikolajewicz and Ernst Maier-Reimer

Max-Planck-Institut für Meteorologie

Bundesstr.55

D-2000 Hamburg 13

F.R.G.

Abstract

We describe results of an experiment in which the Hamburg Large-Scale-Geostrophic ocean general circulation model was driven by a spatially correlated white noise fresh water flux superimposed on the climatological fluxes. In addition to the red noise character of the oceanic response, the model exhibits pronounced variability in a frequency band around 320 years. The centers of action of this oscillation are the Southern Ocean and the Atlantic.

1 Introduction

A major difficulty in the problem of detecting anthropogenic climate modifications in the presence of natural climate variability is the estimation of the natural noise spectrum (Hasselmann, 1979). It is known that this spectrum has significant power in the relevant frequency range of decades to a few centuries (Gates, 1985). A review of known time series is given in Lamb (1977).

For a reliable discrimination between man-made and natural fluctuations the complete spectrum of covariance in the time range under consideration must be known. It is not possible to derive this from historical observations alone. The only feasible way to obtain estimates of the natural covariance spectra is to augment the observations by simulations with models. Since simulations with fully coupled atmosphere-ocean-ice models are at present prohibitively expensive, we investigate in this paper the natural variability with an ocean general circulation model (OGCM). On the time scales of decades to a few centuries the ocean is believed to govern the structure of the probability spectrum through its internal dynamics and through the integration of short term atmospheric fluctuations, which transforms the essentially white noise forcing into a red response spectrum (Hasselmann, 1976).

Although the importance of the ocean for climate fluctuations has been known for a long time (e.g. v.Humboldt, 1845), knowledge about regional details and dynamics of such long-term oscillations is still rather poor. Rossby waves are presumably not slow enough to affect the low frequency part of the spectrum with which we are concerned. Several authors (Stommel, 1961, Rooth, 1982) have argued that the different nature of heat and freshwater fluxes contributing to the net surface buoyancy flux may lead to slow oscillations between two different metastable states. This hypothesis has found support by numerical experiments with the Princeton OGCM (Bryan, 1986) and by further theoretical investigations by Marotzke et al. (1988). Simplified models of such behaviour have been summarised by Welander (1986).

The importance of ocean-atmosphere feedbacks combined with the possible existence of different meta-stable circulation modes for climate change has been stressed in several papers concerned with the Younger Dryas event, the most important climatic fluctuation since the last deglaciation (e.g. Berger and Vincent, 1986 or Broecker et al., 1988). Maier-Reimer and Mikolajewicz (1989) confirmed some of these hypotheses by sensitivity studies with an ocean general circulation model (OGCM).

Müller and Willebrand (1985) have also reported the possibility of another form

of "caballing" oscillation arising from the nonlinear dependence of the density on temperature, salinity and pressure, with a relatively long oscillation period which is related to the time scale of vertical advection. So far, however, there is no experimental evidence of such oscillations in the ocean.

The simplifications underlying many of these theoretical investigations emphasises again the need for an investigation of such phenomena in realistic circulation models. To our knowledge, OGCMs have not previously been applied for this purpose.

In this paper we investigate the natural variability of an OGCM in response to a simulated white noise atmospheric forcing. In the high frequency range of the ocean variability spectrum, the ocean acts as a straightforward integrator without feedback, yielding an ω^{-2} red noise response. For lower frequencies ω , the details of the internal dynamics of the ocean determine the ocean response, and the spectrum can be expected to be more complex (Hasselmann, 1976). Most stochastic forcing models have been formulated in the past for relative simple linear feedback systems enabling analytical or semi-analytical solutions, for example Lemke (1977), Wigley and Raper (1990) for the global ocean, Frankignoul and Hasselmann (1977), Reynolds (1979), and Herterich and Hasselmann (1987) for the surface ocean layers or Lemke et al. (1980) for sea ice. For the global ocean such simple models provide useful estimates of the expected orders of magnitude of oceanic variability but are incapable of capturing possible ocean oscillation modes which could yield strong amplifications in some regions of the variability spectrum and which may be expected to have the strongest influence on climate variability.

We shall describe an experiment in which the Hamburg Large-Scale-Geostrophic OGCM is driven by climatological boundary values of temperature, fresh water and momentum fluxes with a superimposed fresh water flux noise. The noise is represented as a white noise forcing, i. e. with no correlation from month to month (the model timestep) but with coherent spatial structures of approximately 25° correlation scale. The ocean response spectrum is found to have a pronounced peak around 320 years which can be identified with an "eigenmode" of the ocean.

2 The model

The Hamburg Large-Scale-Geostrophic OGCM, whose concept was originally proposed by Hasselmann (1982), is especially designed for the study of slow climatic variations. An implicit integration method permits a time step of 30 days, thus allowing integrations over thousands of years at acceptable computing cost. Basic features of this model are described in Maier-Reimer and Hasselmann (1987). De-

tails are presented in Maier-Reimer et al. (1990b), who discussed the sensitivity of the steady state ocean circulation to different formulations of the upper boundary condition for heat and salt. From a series of experiments with varying boundary conditions they defined a standard run which best reproduces the observed large-scale thermohaline circulation. Further sensitivity and response experiments have been carried out with this model by Maier-Reimer and Mikolajewicz (1989) (sensitivity of the thermohaline circulation to North Atlantic fresh water input), Maier-Reimer et al. (1990a) (response to open isthmus of Panama) and Mikolajewicz et al. (1990) (response to greenhouse warming).

The model is based the conservation laws for heat, salt and momentum (the latter in a linearised form), the full equation of state and the hydrostatic approximation. The global version of the model has a horizontal resolution of 3.5×3.5 degree and 11 vertical layers (centered at 25, 75, 150, 250, 450, 700, 1000, 2000, 3000, 4000 and 5000 m). Topography is included, as well as a one-layer thermodynamic sea ice model with viscous rheology.

The annual cycle is resolved in the model, although in this paper only annual mean values will be shown.

For the wind forcing at the upper boundary the monthly mean wind stress climatology of Hellerman and Rosenstein (1983) was used. The temperature in the surface layer was computed by a Newtonian type coupling to prescribed monthly mean air temperatures derived from the COADS data set (Woodruff et al. 1987), with a coupling coefficient of $40 \text{ W}/(\text{m}^2\text{K})$ (in the absence of sea ice). This yields a time constant of approximately 2 months for a thickness of 50 m for the uppermost layer.

In an initialisation run, the model was driven with a similar Newtonian coupling (with a time constant of 40 days) to the observed climatological annual mean surface salinity (Levitus, 1982). As initial condition, homogenous water with a potential temperature of 2.5°C and with a salinity of 34.5‰ was used. After 10,000 years of integration this run had achieved an almost stationary state with a residual trend of less than $2 \times 10^{-6} \text{ K}/\text{year}$ and $5 \times 10^{-8} \text{‰}/\text{year}$ of salinity in the 4000 m layer. From this run, the effective freshwater flux arising from the coupling to the observed salinity was determined. In the following experiments, this freshwater flux was then taken as boundary forcing acting on the surface salinity (and on the surface elevation), while still retaining the prescribed atmospheric temperature as the temperature boundary condition.

In the absence of a coupled atmospheric model, these "mixed" boundary conditions may be regarded as a reasonable approximate description of the feedback between the ocean and the atmosphere. Anomalies of the sea surface temperature

(SST) are damped out by the resultant anomalous atmosphere-ocean heat fluxes, whereas anomalies in the surface salinities have no influence on the net fresh water flux. Thus anomalies in the salinity distribution have much longer life times than anomalies of the SST. (A convincing example for the lack of atmospheric feedback on the salinity was observed in the seventies, when a large negative salinity anomaly in the Northern Atlantic persisted for at least 14 years, cf. Dickson et al., 1988).

3 The experiment

In a first experiment the model was started from an initial state given by the stationary field from the initialisation run and integrated further with prescribed, non-perturbed freshwater fluxes. After 4000 years of integration the model still exhibited the same circulation as in the initialisation run. This run will be referred to as the control run. The long integration time was needed to ensure that the circulation remained stable after the switch in the salinity boundary condition.

In the stochastic forcing experiment a random forcing in the freshwater flux was than added. The forcing was white in time, had a horizontal correlation of roughly 25 degrees and a globally averaged standard deviation of 16 mm/month. This value correspondes to 20% of the globally averaged annual mean precipitation. (Baumgartner and Reichel 1975).

For the construction of spatially coherent patterns of the freshwater flux we used the first thirty eigenfunctions of the Laplace operator in our grid with the boundary condition of vanishing gradients normal to coasts. The eigenfunctions were obtained by a repeated application of the Ritz procedure, which yields a series of eigenvalues in ascending order. Fig.1 shows as examples the eigensolutions 15, 16, 22 and 23. The structures in the open ocean are similar to those of spherical harmonics. All eigenfunctions were used with equal weights.

Fig. 2 shows the resulting distribution of the standard deviation of the freshwater flux. In the open ocean it is almost constant at a level of 15 mm/month. Towards the coasts the amplitude generally increases. The largest amplitudes are seen in the almost closed basins of Hudson bay and the Mediterranean.

Despite the large variations obtained by this noise forcing, the long term mean state of the circulation remained remarkably close to the state of the control run. Fig. 3 shows the zonally integrated meridional stream function of the Atlantic. (The lack of meridional boundaries makes this quantity meaningless south of 30°S). The basic

feature of the Atlantic meridional flow is a northward inflow from the Southern Ocean of 17 Sverdrup (Sv) in the upper 1.5 km which sinks in the North Atlantic to form the North Atlantic deep water (NADW). The flow leaves the Atlantic at depths of 2 to 3 km. The deeper inflow of Antarctic bottom water (AABW) has a strength of 6 Sv. At the surface, wind driven Ekman cells are seen. This pattern of meridional overturning is consistent with the Atlantic segment of the global "conveyor belt" (Gordon, 1986, see also Wüst, 1935). From the analysis of data for temperature, salinity, nutrients and potential vorticity, Roemmich and Wunsch (1985) estimate of a meridional thermohaline circulation of 17 Sv (at 24°N).

The north-south section of salinity through the western Atlantic (fig. 4) follows the structure of the flow patterns. On their way to the north the salinity of the surface waters increases due to evaporation at the surface. This is responsible for the high salinity of the southward flowing NADW after the surface waters have sunken to depths of 2 to 3 km. At 1 km depth, fresh Antarctic intermediate water from the Southern Ocean flows northward. The bottom layer shows an inflow of still fresher and colder AABW from the Southern Ocean.

Fig. 5 shows time series of some integral parameters which characterize the instantaneous state of the circulation during the stochastic forcing experiment. All represent annual mean values without further filtering. The first panel shows an input time series, the integral of the net fresh water flux over the entire ocean south of 30°S. The short term variability is dominant and the frequency spectrum (shown in fig. 6) is white, as it should be. All other time series represent the response of the ocean to this forcing.

The ocean circulation exhibits pronounced but irregular oscillations with a typical time scale of 320 years. This signal stands out most clearly in the time series of the strength of the Antarctic circumpolar current (ACC). The range of variability exceeds 100 Sv. The mean value is 118 Sv, compared to 126 Sv for the initialisation run (Maier-Reimer et al. 1990b). The mean measured transport through Drake passage inferred from 3 year records of pressure gauges is 123 ± 10 Sv (Whitworth and Peterson 1985). The spectrum of the simulated ACC variability is shown in fig. 3. For comparison three spectra of the simplest stochastic climate model representing first order Markov processes with time constants of 50 and 500 years and infinite time constant (simple integrator) are shown too. For time scales less than 30 years all spectra coincide, but for longer time scales the spectrum for our simulation shows a pronounced peak at 320 years, well above the simple ω^{-2} integrator red noise spectrum, which must clearly be attributed to the more complex internal dynamics of the model ocean.

The integral of the atmosphere-ocean heat exchange (positive values indicate heat transfer into the ocean) in the Southern Ocean is highly correlated with the

strength of the ACC. One of the first successful applications of an OGCM was indeed the demonstration that the strength of the ACC is strongly dependent on the temperature structure (which controls the atmosphere-ocean heat transfer) through the interaction of density and topographic gradients (Cox, 1975). During intervals of weak heat loss to the atmosphere the deep water production is smaller than usual. This reduces the south-north density gradient and thereby also the geostrophic velocities, resulting in a weak transport of the ACC. The atmosphere-ocean heat exchange in the North Atlantic (north of 30°N including the Arctic) shows the same signal, though it is considerably weaker. The heat exchange in this region is inversely correlated with the heat fluxes of the Southern Ocean.

The figures indicate that the ocean exhibits an "eigenmode" with a typical time scale of 320 years which connects the polar regions and is asymmetric with respect to the equator. The strongest effects are located around Antarctica. This is presumably only one of several modes of oscillation, but we will restrict ourselves in this paper to describe this particular mode as perhaps a typical example of long-term variability in the ocean.

The mode does not appear as a continuous oscillation but rather in the form of discrete events, in analogy with El Niño. In order to investigate the nature of this event in more detail we constructed composites, using the minima of the ACC (indicated by the vertical lines in fig 5) as the reference times. The choice of reference time is essentially arbitrary, our choice lies about in the middle of an event and therefore should not be interpreted as the triggering time.

The event pattern will be described in terms of the salinity anomaly. Since the salinity is free at the surface - in contrast to the temperature - and it is affected directly by the variable forcing, and the salinity may therefore be expected to be the key variable.

Fig. 7 shows the time evolution of the salinity anomaly during the event in a sequence of snapshots. Each panel represents an average over 20 years.

Fig. 7a shows the state 160 years (or half a period) before the reference time. The strong positive anomaly at the surface in the Weddell Sea is an indicator of active deep water formation. In the upper ocean, the positive anomaly extends northwards to 40°N. The Arctic surface waters and the deep Atlantic waters are relative fresh. The negative anomaly has a maximum at 4 km depth near the equator.

During the evolution of the event the fresh water moves southward and rises to the surface in the Weddell Sea. It begins to affect the deep water production there at $t=-80$ years. The deep water formation is suppressed by the low salinities at

the surface. In this stage a positive feedback mechanism is acting: the negative anomaly is amplified by the longer exposure time of the stabler surface waters to the fresh water fluxes from the atmosphere and the suppressed supply of salty waters from below.

The negative anomaly then spreads northward in the upper ocean with the mean thermohaline circulation. At $t=80$ years, deep convection begins again in the Weddell Sea, and the anomaly has reached the production zone of NADW and is starting to enter the deep Atlantic, where it spreads southward.

At $t=160$ years a situation very similar to that of the first picture is reached, in which the negative anomalies have attained a maximum in the deep Atlantic close to the equator.

The positive anomaly which is located in the upper Southern Ocean at $t=-160$ years moves northward with the mean circulation, starts to enter the NADW 80 years later and then spreads southward in the deep Atlantic. At $t=0$ the deep Atlantic is filled with water masses saltier than usual. The positive anomaly then moves southward and rises to the surface in the Weddell Sea, where deep water formation starts again at $t=40$ years. The anomaly is amplified due to the increased supply of salty water from below and the relative short exposure to the net precipitation. The anomaly spreads northward in the upper ocean and finally reaches 40° N again.

This example of an eigenmode of the ocean circulation has no similarity with the standard linear modes for an ocean at rest. It corresponds to an advected dipole disturbance which is transported by the mean thermohaline circulation of the Atlantic, the upper branch moving northward and the lower branch southward with the NADW. On its way, the poles of the anomaly affect deep water formation and thus gain strength by changes in the time of exposure to the net precipitation in polar regions and by changes in the entrainment of salty water from intermediate depths. The amplification is most effective in the Southern Ocean.

The characteristic time for this process is approximately 320 years. This agrees fairly well with the overall flushing time of the Atlantic, which may be estimated as 400 years from the ratio of the volume to the outflow (at 30° S).

Since the oscillation period is determined by the advective time scale of the Atlantic circulation, the time scale of the corresponding mode for different global climate states - if it still exists - can be expected to be highly variable. Thus for periods when the mean thermohaline circulation was significantly different from the present - e.g. during the time of the last glacial maximum (Broecker et al. 1985) - the oscillation pattern would have been strongly modified.

Our experiment raises several questions. The first and most important is obviously, whether this eigenmode occurs in the real ocean. If so, the simulated variations in the ocean-atmosphere heat exchange at high latitudes should be detectable in climatic records. From existing long-term data records we can only conclude that there is indeed some variability in the frequency ranges discussed here. But whether this is related to the pattern described here is impossible to decide. Other open questions are the propagation of this pattern around Antarctica, the influence of a more realistic atmospheric feedback and the dependence on the amplitude of forcing, which must be expected to be nonlinear due to the near surface amplification connected with the basically nonlinear process of deep water formation.

4 Conclusion

In an OGCM forced with white noise, the internal dynamics of the ocean strongly influences the variability on time scales longer than a few decades. The most pronounced example of this variability is a dipole anomaly advected by and interacting with the mean thermohaline circulation of the Atlantic, with a mean advection period of 320 years. We suggest that oscillations of this type may contribute significantly to natural climatic variability on these time scales.

5 Acknowledgements

Discussions with Klaus Hasselmann helped to improve this paper substantially. We gratefully acknowledge the assistance of Peter Wright in carefully reading this manuscript and Marion Grunert for drawing some of the figures.

6 References:

- Baumgartner A, Reichel E (1975) *Die Weltwasserbilanz*. Oldenbourg Verlag Muenchen, 179 pp.
- Berger WH, Vincent E (1986) *Sporadic shutdown of North Atlantic deep water production during the Glacial-Holocene transition?* Nature 324; 53-55.
- Broecker WS, Peteet D, Rind D (1985) *Does the ocean-atmosphere system have more than one stable mode of operation?* Nature 315; 21-26.
- Broecker WS, Andree M, Wolfli W, Oeschger H, Bonani G, Kennett J, Peteet D (1988) *The chronology of the last deglaciation: implications to the cause of the Younger Dryas event*. Paleoceanography 3,1;1-19.
- Bryan F (1986) *High latitude salinity effects and interhemispheric thermohaline circulations*. Nature 305; 301-304.
- Cox M (1975) *A baroclinic Numerical Model of World Ocean*. In Numerical Models of Ocean circulation, National Academy of Sciences, Washington, pp 107-120.
- Dickson RR, Meincke J, Malmberg S-A, Lee AJ (1988) *The "Great Salinity Anomaly" in the Northern North Atlantic 1968-1982*. Prog. Oceanog. 20; 103-151.
- Frankignoul C, Hasselmann K (1977) *Stochastic climate models, Part II: Application to sea-surface temperature anomalies and thermocline variability*. Tellus 29; 289-305.
- Gates WL (1985) *Modelling as a means of studying the climate system*. in MacCracken MC, Luther FM (eds.) Projecting the climatic effects of increasing carbon dioxide. DOE/ER-0237, p. 57-79.
- Gordon AL (1986) *Interocean exchange of thermocline water*. J. Geoph. Res. 91; 5037-5046.
- Hasselmann K (1976) *Stochastic climate models, Part I, Theory*. Tellus 28, 6, 473-485.
- Hasselmann K (1979) *On the signal-to-noise problem in atmospheric response studies*. Meteorology of Tropical Oceans, Royal Met. Soc.;251-259.

- Hasselmann K (1982) *An ocean model for climate variability studies*. Progr. Oceanogr. 11; 69-92.
- Hellerman S, Rosenstein M (1983) *Normally monthly wind stress over the world ocean with error estimates*. J. Phys. Oceanogr. 13; 1093-1104.
- Herterich K, Hasselmann K (1987) *Extraction of Mixed Layer Advection Velocities, Diffusion Coefficients, Feedback Factors and Atmospheric forcing Parameters from the Statistical Analysis of North Pacific SST Anomaly Fields*. J. Phys. Oceanogr. 17; 2145-2156.
- von Humboldt A (1845) *Kosmos. Entwurf einer physischen Weltbeschreibung*. Erster Band. Cotta'scher Verlag, Stuttgart und Tübingen, pp 453.
- Lamb HH (1977) *Climate: present past and future*. Vol. 2. Methuen & Co London, pp 835.
- Levitus S (1982) *Climatological Atlas Of the World Ocean*. NOAA professional Paper 13, Rockville Md.
- Lemke P (1977) *Stochastic climate models, part 3, application to zonally averaged energy models*. Tellus 29; 385-392.
- Lemke P, Trinkl EW, Hasselmann K (1980) *Stochastic Dynamic Analysis of Polar Sea Ice Variability*. J. Phys. Oceanogr. 10; 2100-2120.
- Maier-Reimer E, Hasselmann K (1987) *Transport and storage of CO₂ in the ocean - an inorganic ocean-circulation carbon cycle model*. Climate Dynamics 2; 63-90.
- Maier-Reimer E, Mikolajewicz U (1989) *Experiments with an OGCM on the Cause of the Younger Dryas*. in Ayala-Castanares A, Wooster W, Yanez-Arancibia A (eds.) Oceanography 1988. UNAM Press Mexico, pp 87-100.
- Maier-Reimer E, Mikolajewicz U, Crowley T (1990a) *Ocean GCM sensitivity experiment with an open Central American Isthmus*. submitted to Paleoceanography.
- Maier-Reimer E, Mikolajewicz U, Hasselmann K (1990b) *On the sensitivity of global ocean circulation to surface forcing*. (in prep.)
- Marotzke J, Welander P, Willebrand J (1988) *Instability and multiple steady states in a meridional-plane model of the thermohaline circulation*. Tellus 40A; 162-172.
- Mikolajewicz U, Santer B, Maier-Reimer E (1990) *Ocean response to greenhouse*

warming. (submitted to Nature)

Müller P, Willebrand J (1985) *Compressibility effects in the thermohaline circulation: a manifestation of the temperature-salinity mode*. Deep-Sea Research 33; 559-571.

Reynolds RW (1979) *A stochastic forcing model of sea surface temperature anomalies in the North Pacific and North Atlantic*. Climatic Research Institute, Rep. No. 8, Oregon State University.

Roemmich D, Wunsch C (1985) *Two transatlantic sections: meridional circulation and heat flux in the subtropical North Atlantic Ocean*. Deep-Sea Research 32; 619-664.

Rooth C (1982) *Hydrology and ocean circulation*. Progr. Oceanogr. 11; 131-149.

Stommel H (1961) *Thermohaline convection with two stable regimes of flow*. Tellus 13; 224-230.

Welander P (1986) *Thermohaline effects in the ocean circulation and related simple models*. in Willebrand J, Anderson DLT (eds.) Large-Scale Transport Processes in Oceans and Atmosphere, 163-200, D. Reidel.

Whitworth T, Peterson RG (1985) *Volume Transport of the Antarctic Circumpolar Current from Bottom Pressure Measurements*. J. of Phys. Oceanogr. 15; 810-816.

Wigley T, Raper S (1990) *Natural variability of the climate system and detection of the greenhouse effect*. In Schlesinger ME (ed.) Proceedings of DOE Workshop on Greenhouse-Gas-Induced Climatic Change (in press).

Woodruff SD, Slutz RJ, Jenne RL, Steurer PM (1987) *A comprehensive ocean-atmosphere data set*. Bull. Am. Soc. 68; 1239-1250.

Wüst G (1933) *Schichtung und Zirkulation des Atlantischen Ozeans. Das Bodenwasser und die Gliederung der Atlantischen Tiefsee*. In Wissenschaftliche Ergebnisse der Deutschen Atlantischen Expedition auf dem Forschungs- und Vermessungsschiff "Meteor" 1925-27, 6: 1. Teil, 1, pp 106 (in German).

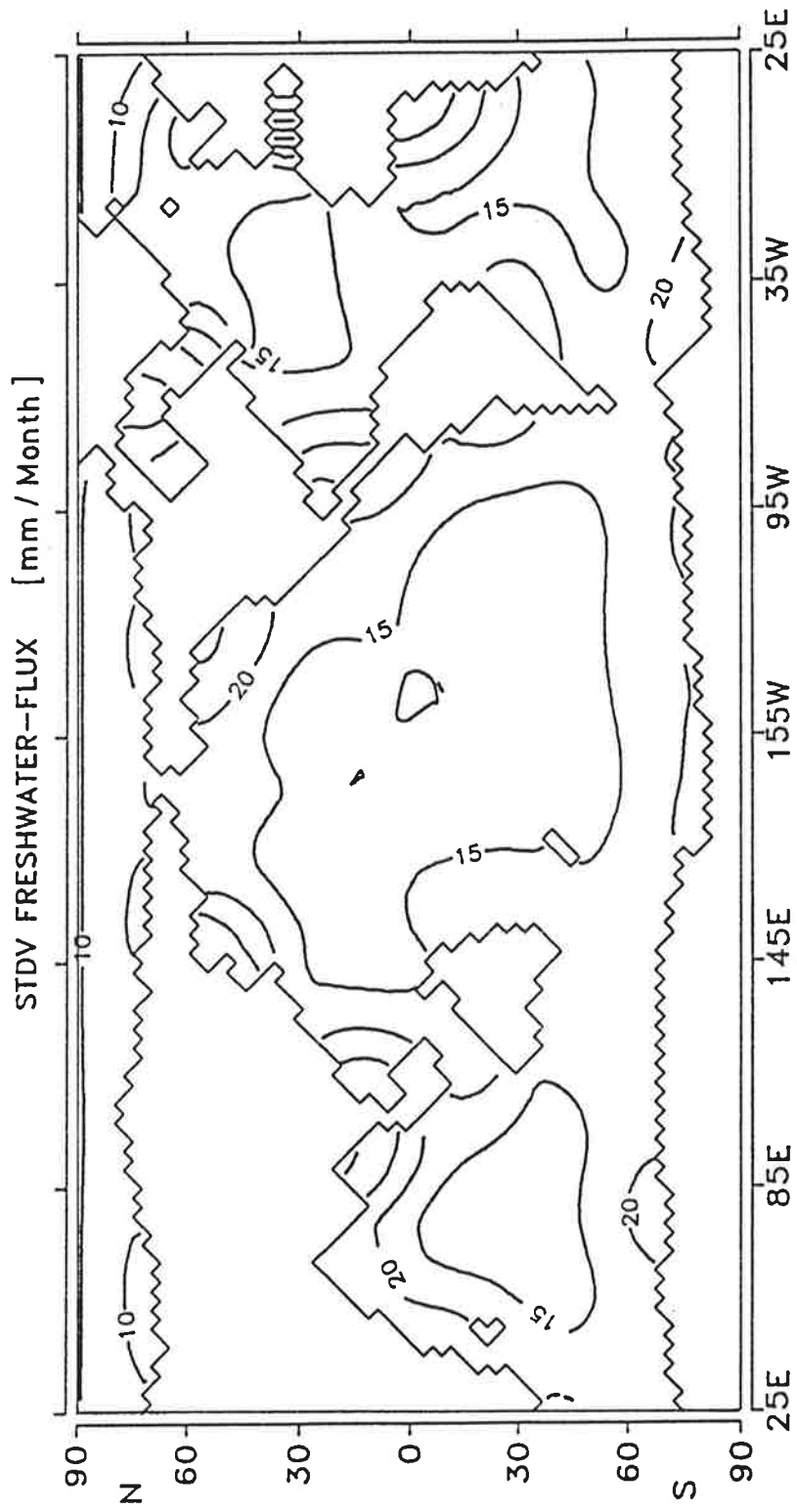


fig. 1

Standard deviation of the noise added to the climatological fresh water fluxes.

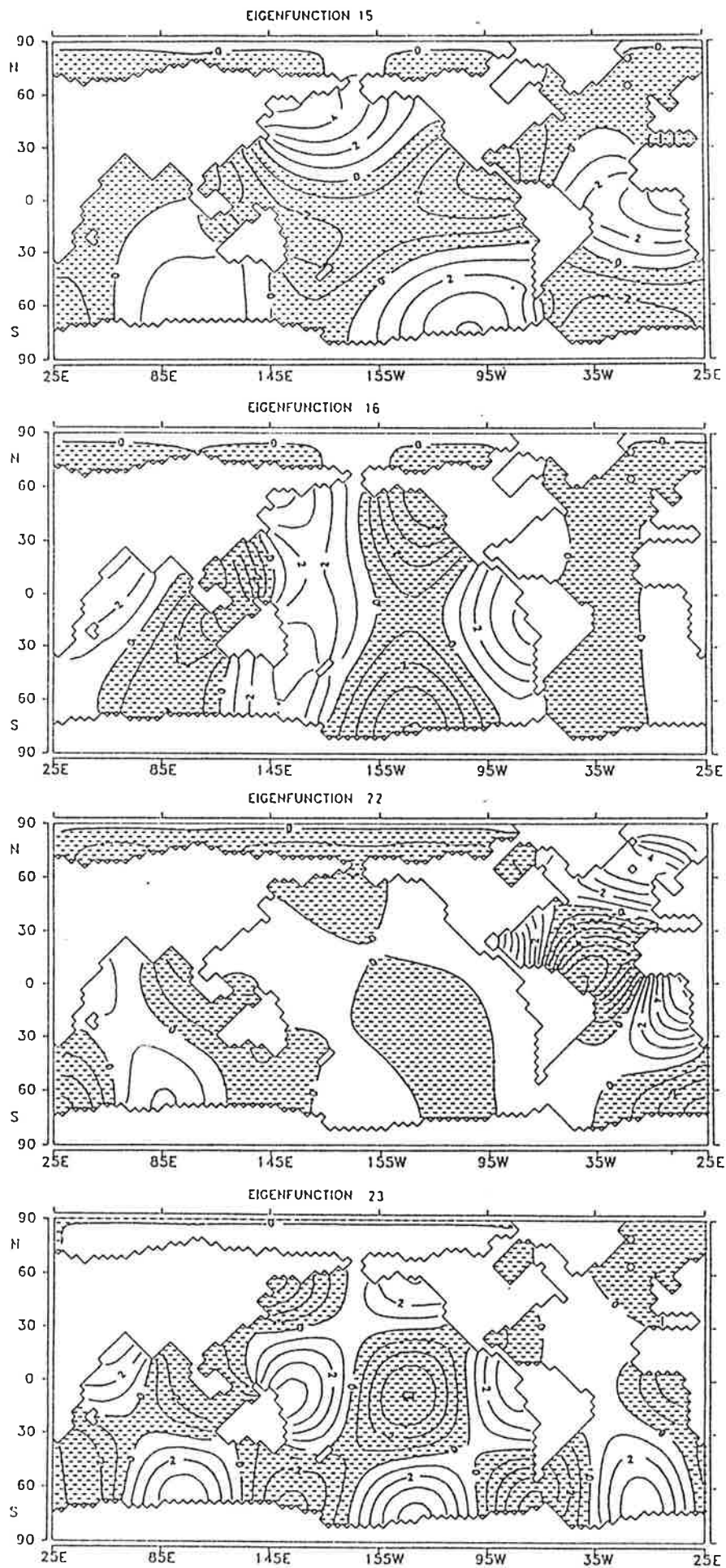


fig. 2

Examples of the eigenfunctions of the inverse Laplace operator used as forcing functions for the noise. Displayed are the eigenfunctions 15, 16, 22 and 23. The units are arbitrary, stippled areas are negative.

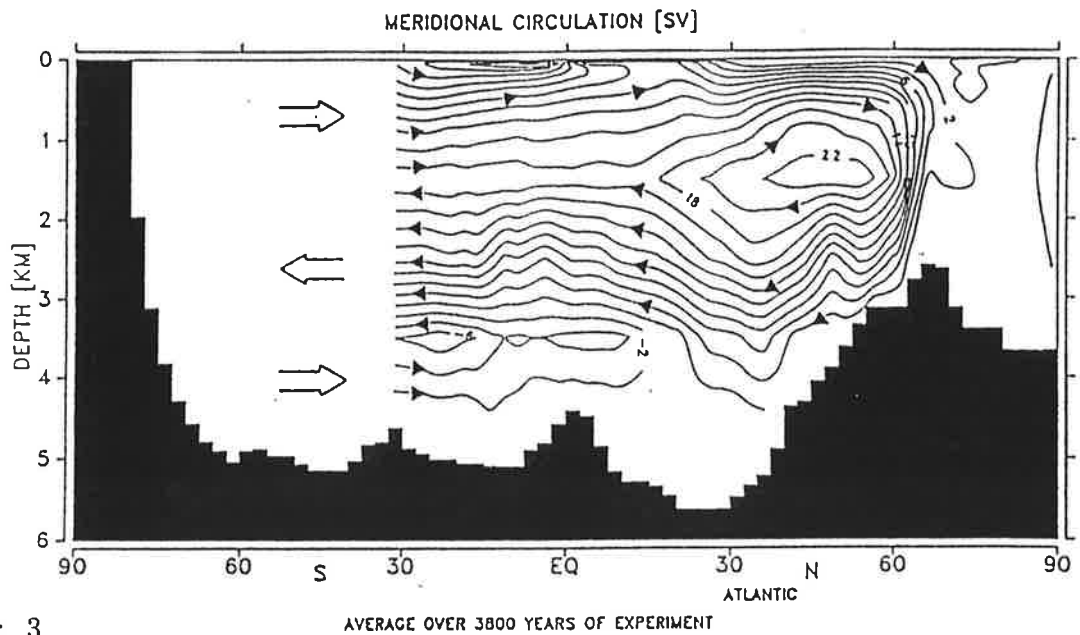


fig. 3

Zonally integrated mean meridional mass transport streamfunction of the Atlantic averaged over the 3800 years of integration. Because of the lack of solid meridional boundaries south of 30 °S this quantity is meaningless in these latitudes. The arrows indicate the direction of the flow, contour interval is 2 Sverdrup.

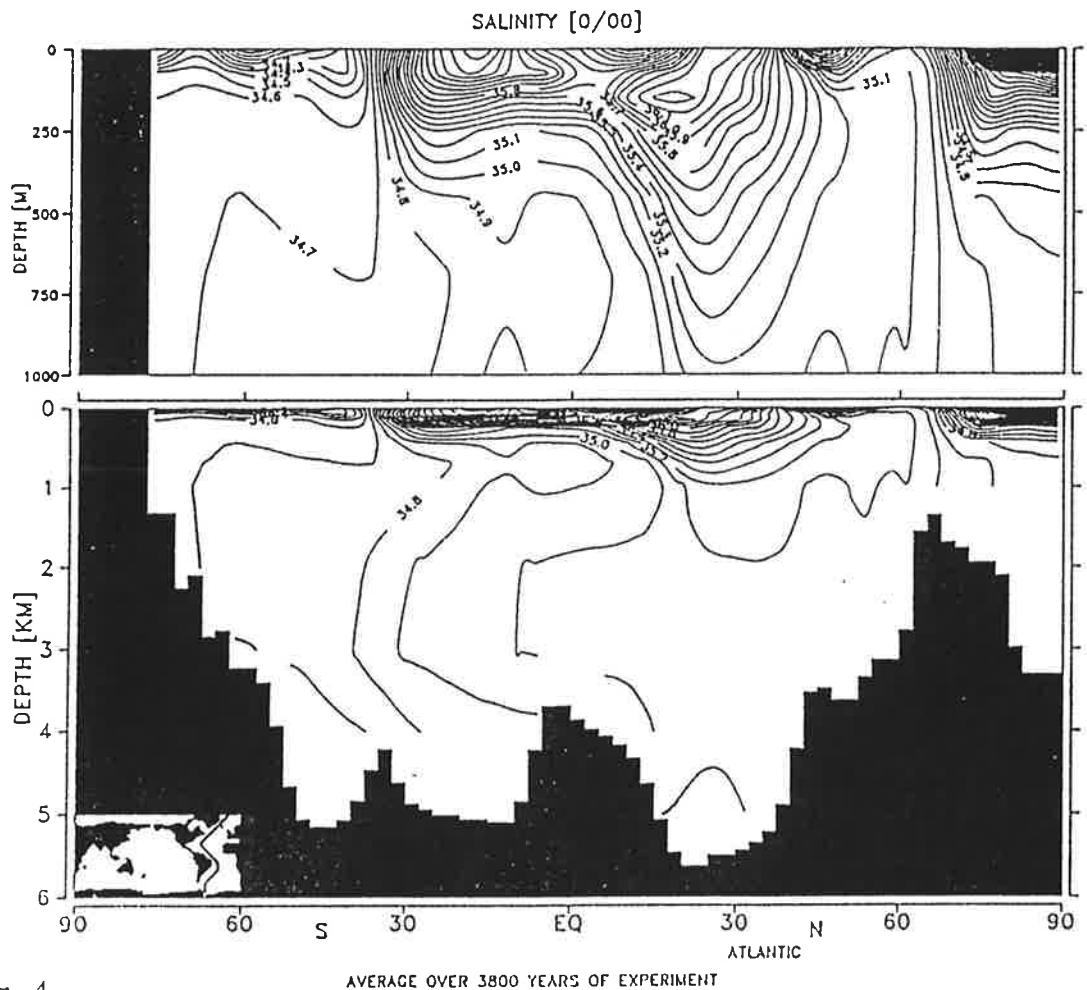


fig. 4

Mean salinity (averaged over the 3800 years of the experiment) section through the western Atlantic. The exact location of the section is shown in the insert. The upper panel shows an enlargement of the upper 1000 m. The different water masses as AABW, NADW and Antarctic Intermediate waters (AAIW) are detectable. The contour interval is 0.1 psu.

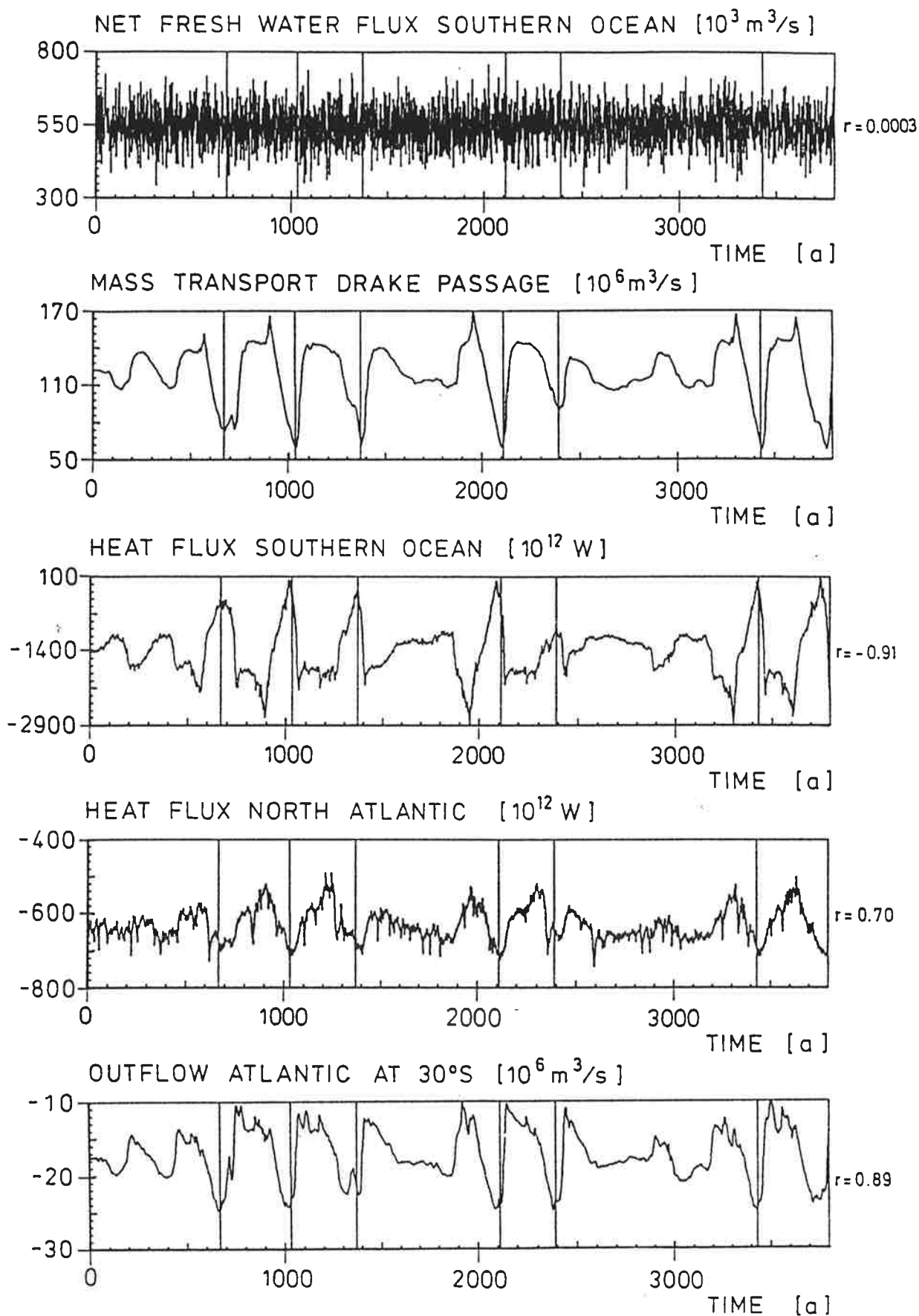


fig. 5

Annual mean time series of net freshwater flux in the Southern Ocean (south of 30°S), the mass transport through Drake Passage, the atmosphere-ocean heat exchange (heat loss of the ocean gives negative values), in the Southern Ocean and in the North Atlantic (Atlantic north of 30°N and Arctic) and the outflow of NADW at 30°S from the Atlantic to the Southern Ocean, negative values indicating flow to the south. The vertical lines represent the reference times of the defined events used for the composites.

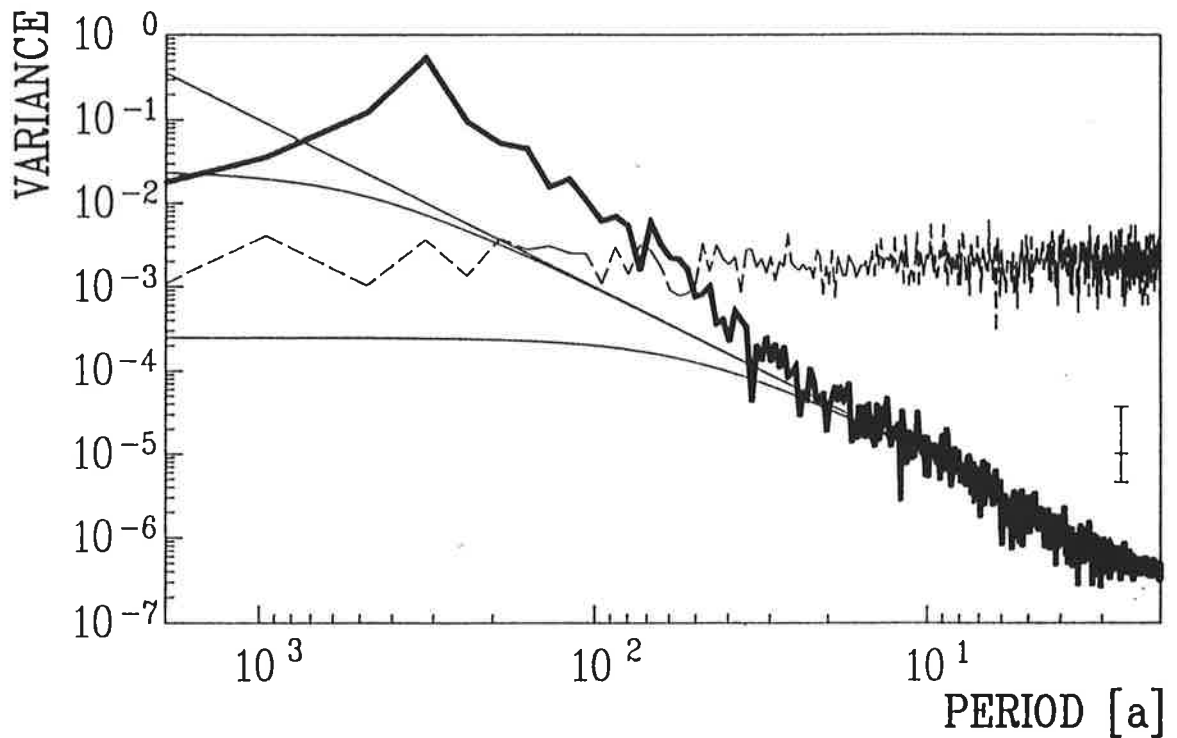


fig. 6

Variance spectrum of the mass transport through Drake Passage and the net freshwater flux of the Southern Ocean (dashed line). Data are scaled by their standard deviation. The thin lines represent the results to be expected from simple linear stochastic climate models with time constants of 50 years, 500 years and infinite. For periods less than 30 years the shape of the spectrum can be approximated by a stochastic climate model, whereas for longer periods the spectral shape is significantly different due to the internal dynamics of the ocean. The bar indicates the 95% confidence interval.

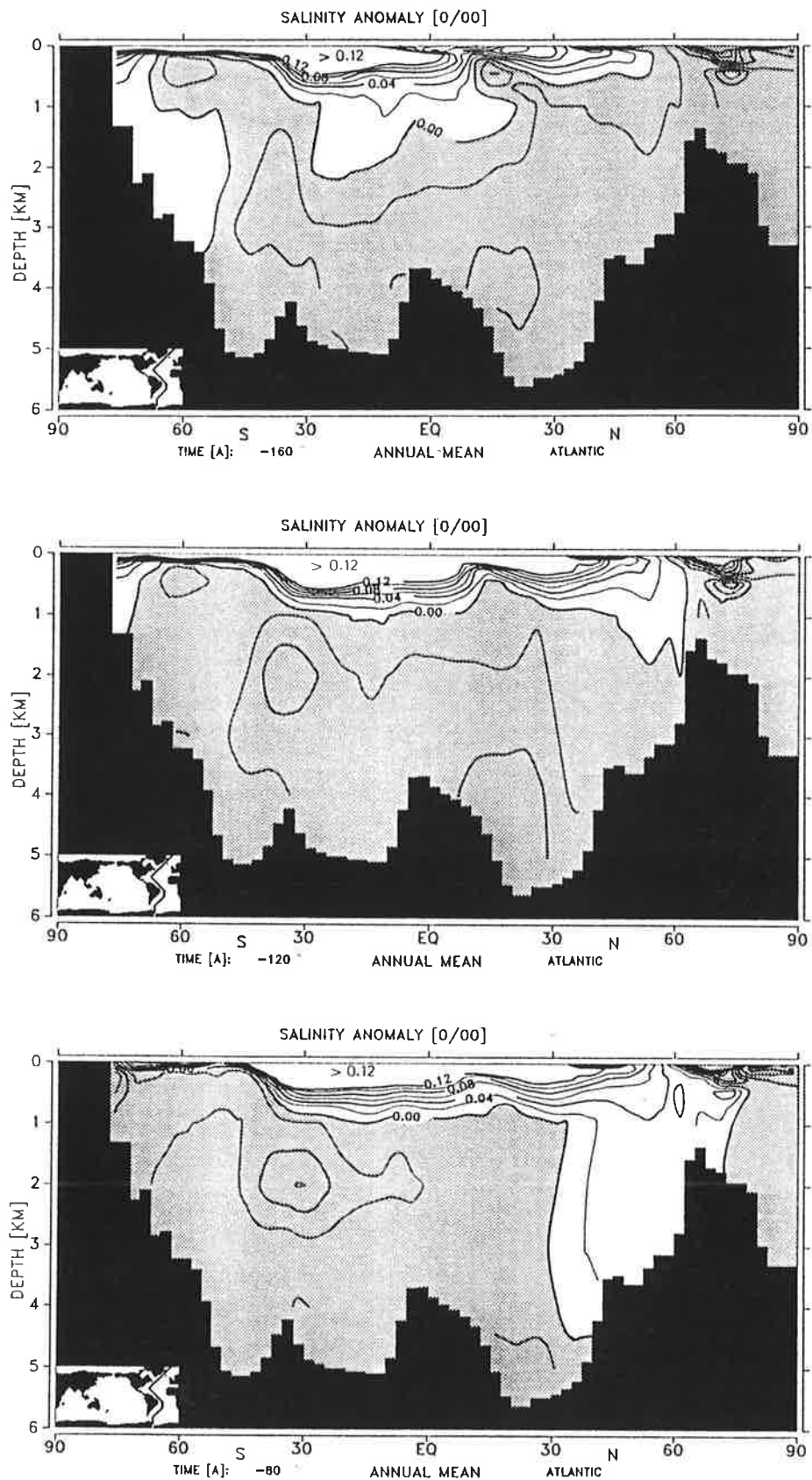


fig. 7 a-c

Salinity anomalies of the composites on a north-south section through the Western Atlantic (mean state and location shown in fig. 4). Each graph represents an average over 20 years. Numbers give the time relative to the reference time in years, the distance between subsequent snapshots is 40 years. A clockwise propagation of the anomalies with the mean thermohaline circulation of the Atlantic is obvious. The contour interval is 0.02 ‰ . Isolines are plotted for the interval between -0.012 and 0.012 . Shading indicates negative values.

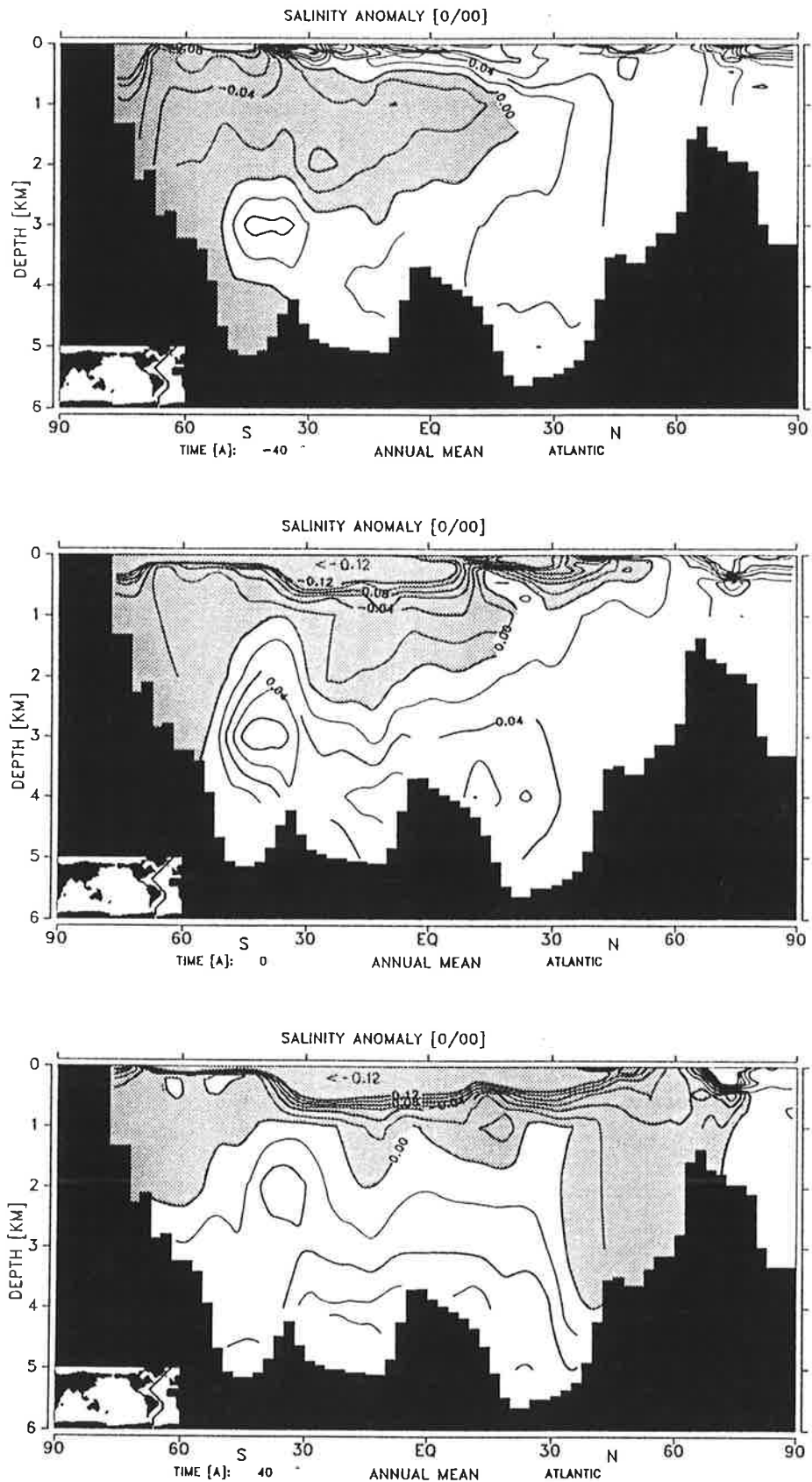


fig. 7 d-f

Salinity anomalies of the composites on a north-south section through the Western Atlantic (mean state and location shown in fig. 4). Each graph represents an average over 20 years. Numbers give the time relative to the reference time in years, the distance between subsequent snapshots is 40 years. A clockwise propagation of the anomalies with the mean thermohaline circulation of the Atlantic is obvious. The contour interval is 0.02 ‰. Isolines are plotted for the interval between -0.012 and 0.012. Shading indicates negative values.

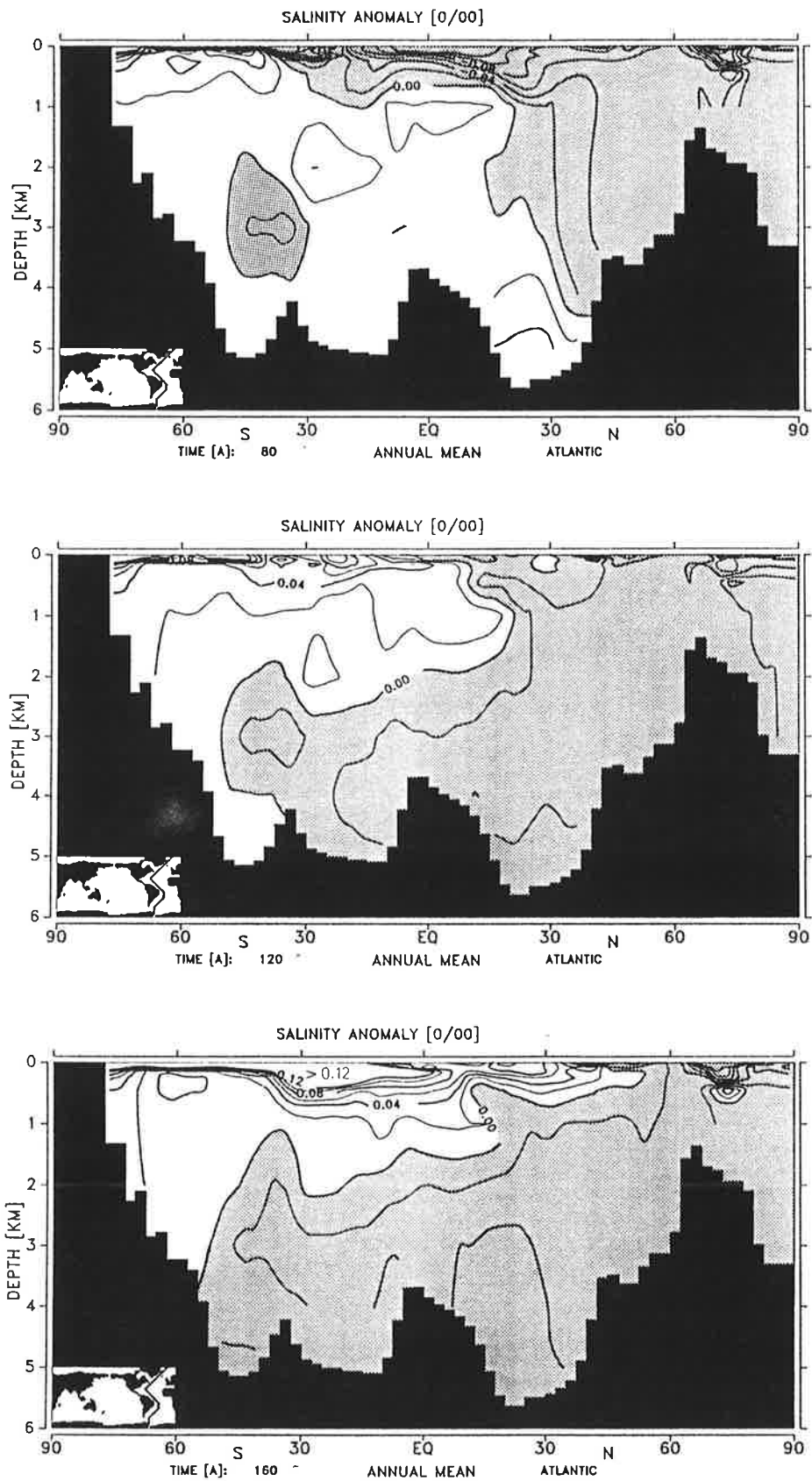


fig. 7 g-i

Salinity anomalies of the composites on a north-south section through the Western Atlantic (mean state and location shown in fig. 4). Each graph represents an average over 20 years. Numbers give the time relative to the reference time in years, the distance between subsequent snapshots is 40 years. A clockwise propagation of the anomalies with the mean thermohaline circulation of the Atlantic is obvious. The contour interval is 0.02 ‰ . Isolines are plotted for the interval between -0.012 and 0.012 . Shading indicates negative values.